The Metaplectic Sampling of Quantum Engineering

Walter J. Schempp

Lehrstuhl für Mathematik I, University of Siegen, 57068 Siegen, Germany

Abstract. Due to photonic visualization, quantum physics is not restricted to the microworld. Starting off with synthetic aperture radar, the paper provides a unified approach to clinical magnetic resonance tomography and the bacterial protein dynamics of structural microbiology. Its mathematical base is harmonic analysis on the three–dimensional Heisenberg Lie group with associated nilpotent Heisenberg algebra Lie(N).

Keywords: Heisenberg Lie group, Heisenberg nilpotent Lie algebra, metaplectic representation, data sampling, synthetic aperture radar imaging, magnetic resonance tomography, bacterial protein dynamics, flagellar motor, rotational switching, tracking of chemotaxis

1. THE HEISENBERG LIE GROUP

Consider a particle in a one–dimensional space. Its quantum mechanical description is obtained by introducing variables suggested by the classical theory in its Hamiltonian form. These variables which are *not* numbers and do not commute in general, form an algebraic structure generated by two basic self–adjoint elements P and Q satisfying the Heisenberg commutation relation

$$\boxed{[P,Q]=-i}$$

where the bracket denotes the commutator. The elements P and Q are supposed to be represented by self–adjoint operators in Hilbert space. These operators are unbounded and this might involve domain problems which Werner Karl Heisenberg (1901 to 1976) was unable to appreciate. Heisenberg did not recognize the difference between bounded and unbounded linear operators in infinitely dimensional Hilbert spaces, which is at the origin of distribution theory created by Laurent Schwartz (1915 to 2002). Similarly, Erwin Schrödinger (1887 to 1961) strongly believed that even thought–experiments with just one electron or atom or small molecule invariably entail ridiculous consequences. From this opinion, the advances of present–day quantum physics and quantum engineering can be easily recognized.

The three–dimensional Heisenberg Lie group N with one–dimensional center implements the Heisenberg commutation relation. As a central extension of the symplectic plane $\mathbf{R}\oplus\mathbf{R}$ it is isomorphic to the direct sum $\mathbf{C}\oplus\mathbf{R}$ under the multiplication law

$$\boxed{(w_1,z_1)(w_2,z_2)=\left(w_1+w_2,z_1+z_2+\frac{1}{2}\Im\left(\bar{w}_1w_2\right)\right)}$$

for elements $(w,z)\in\mathbf{C}\oplus\mathbf{R}$. The fact that the one–dimensional center $\{(0,z)|z\in\mathbf{R}\}$ of N is non–trivial implies dramatic deviations from commutative Fourier analysis of signal analysis and communication theory. Roughly speaking, the Fourier transform and the Fourier cotransform on the real line $\mathbf{R}$ have to be replaced by equivalence classes of irreducible unitary linear representations of N and their contragredient siblings. These equivalence classes can be visualized by inhomogeneous planes transversal to the central axis $\{(0,z)|z\in\mathbf{R}\}$, and symmetrically organized with respect to the origin so that they are tangent to the two–dimensional Bloch sphere $\mathbf{S}_2$ of nuclear magnetic resonance spectroscopy. The contact points of the Bloch sphere $\mathbf{S}_2=\mathrm{SO}(3,\mathbf{R})/\mathrm{SO}(2,\mathbf{R})$ allow to coherently control the nuclear spin choreography: Its north pole represents the spin–up state $\uparrow$, its south pole the spin–down state $\downarrow$.

The symmetries associated with the so–called coadjoint orbit picture of N in the vector space dual of its Lie algebra, the real Heisenberg algebra Lie(N), is two–fold. In the longitudinal direction it is represented by the Galois group $\mathrm{Gal}_{\mathbf{R}}\mathbf{C}$ which acts in binary terms by reflecting the central axis. In the transverse direction it is represented by the metaplectic group $\mathrm{Mp}(1,\mathbf{R})$ which acts as a two–fold cover of the unimodular Lie group $\mathrm{SL}(2,\mathbf{R})$ by letting the one–dimensional center pointwise fixed.

The main mathematical tool for a unified approach to quantum holographically data organizations is the three–dimensional real Heisenberg Lie group N which allows to bridge the gap between abelian and nonabelian harmonic analysis by showing how various important filtering results in abelian harmonic analysis may be enriched through an interpretation in terms of the Heisenberg group N and its nilpotent Lie algebra, the Heisenberg algebra Lie(N). Obviously, it needs some habituation to get familiar with these mathematical concepts. However, the broad range of ensuing results makes it worthwhile to think in the broad category of holographically encoded data organizations.

Unfortunately, harmonic analysis on the Heisenberg

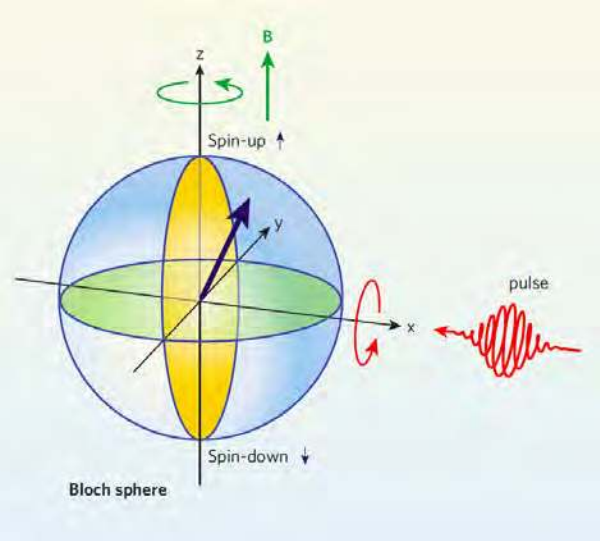

FIGURE 1. Nuclear spin excitation procedure of magnetic resonance tomography. The Bloch sphere $\mathbf{S}_2$ of nuclear magnetic resonance spectroscopy allows to control the nuclear spin choreography in a strong magnetic field B of homogeneous density.

Lie group N is not a very popular research subject today. Why has a mathematical object with applications of such a wide spectrum gone relatively unnoticed until recently? One can only speculate. Hermann Weyl (1885 to 1955), one of the pioneers in introducing the Heisenberg group into quantum physics, overlooked the natural occurrence of the Heisenberg group, exploitation of which yields results which one feels he would have liked very much. An obstacle to the appreciation of the common underlying structure may have been the very diversity of the topics, for detection of its presence in one place need not suggest its presence elsewhere. Indeed, investigators in one field may very well never have been aware that the Heisenberg Lie group had been found in some area not seemingly related to theirs ([8], [9]).

2. SYNTHETIC APERTURE RADAR

In 1903, a mere 15 years following the seminal studies of Heinrich Hertz (1857 to 1894) on the generation, reception, and scattering of electromagnetic waves, the engineer Christan Hülsmeyer (1881 to 1957) demonstrated a ship collision avoidance radar system which he later patented. The range of the first remote sensing system was about 3 km. Although there was a demand for such remote sensing modalities, time was not mature enough to recognize the importance of Hülsmeyer's discovery. It needed several generations of scientists after Hülsmeyer's breakthrough to evaluate the information contents of the sophisticated echo or response signals generated by remote sensing modalities other than radar systems. Due to theoretical insights into the application of the Hanbury Brown–Twiss phenomenon of photon bunching to astrophysics, the link between radar technology and quantum engineering has been established. Important technological advances in varied applications of photonics have made the breadth of this link by far more apparent. They demonstrated that quantum physics and quantum engineering are not restricted to the visualization of the microworld.

Astronomy is considered to be the most ancient of all the sciences. The role of planetary exploration and imaging is quite unusual in the history of science: A research subject that was created almost instantaneously when an esoteric speciality was elevated to prominence during the space race. One of the culminations in the development of remote sensing systems represented the spaceborne Magellan's synthetic aperture radar which has penetrated the Venusian clouds to furnish 100–meter resolution, false–colour images. Once considered the earth's twin because of its similar size and mass, the planet Venus which is completely shrouded in dense clouds is now known as strikingly different. Indeed, a carbon dioxide atmosphere caused a runaway greenhouse effect that today produces scorching temperatures that induced nearly all of the planet's water to escape. Venus' thick clouds are made of sulphuric acid, not water droplets like the earth's clouds. The planet's surface is surprisingly young, and volcanoes are widespread. Lava flooding is thought to have obliterated most surface features only 800 million years ago. The earth's nearest planetary sibling presents an impressive example of how a planet's surface conditions are sensitive to its atmospheric content. It demonstrates that advances in high technology enhanced considerably the range of our knowledge.

Radar systems have been operated since the early 1930s, but with rapidly increasing sophistication of technology. Nearly 60 years have passed since Carl A. Wiley first observed that a side–looking radar system can considerably improve its azimuth resolution by utilizing the Doppler spread of the echo signal. In the ensuing years, a flurry of activity followed, leading toward steady advancement in performance of both the sensor and the echo signal processor technology. Although much of the early work on remote sensing was aimed toward detection and tracking of moving targets, the potential for utilizing this technology as a tomographic imaging modality for scientific applications was widely recognized, and an apex in the development of high resolution imaging modalities has been achieved by synthetic aperture radar systems of airborne or spaceborne platforms. Later on, orbital spin geometry, fast nuclear spin–echo strategies, and photon–echo formation opened new horizons to innovative non–invasive tomographic imaging modalities

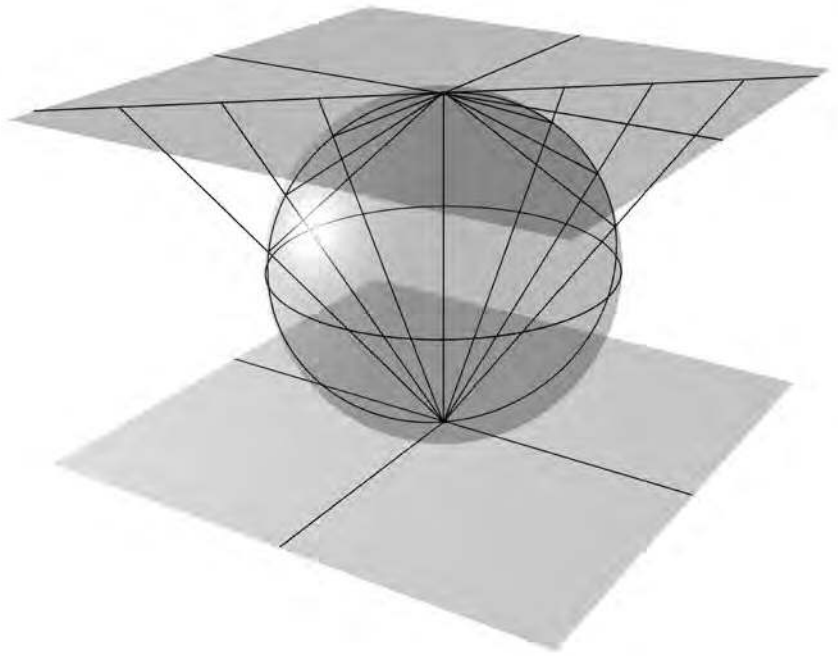

FIGURE 2. The axisymmetric and time asymmetric coadjoint orbit picture of the Heisenberg Lie group N in the three–dimensional real projective space visualizes pairs of non–equivalent symplectic tomographic slices. They are at the origin of the quantum eraser principle of quantum entanglement. The circular boundary of the closed disc in the equatorial plane $\nu = 0$ indicates the points of angular momentum transfer. The symmetry in the longitudinal direction is represented by the Galois group $\mathrm{Gal}_{\mathbf{R}}\mathbf{C}$ whereas in the transversal direction it is represented by the metaplectic group $\mathrm{Mp}(1, \mathbf{R})$.

FIGURE 3. Three–dimensional projective geometry: Rotations induced by the symplectic structure of the planar detector. The exposure time is 10 h.

FIGURE 4. Spaceborne Magellan's synthetic aperture radar observations reveal the planet's Venus landscape by mapping radar mosaics onto a computer–simulated two–dimensional sphere $\mathbf{S}_2$ in the three–dimensional real projective space. The global radar view of the shrouded surface of Venus is centered at 180^{o} east longitude. Remarkably, Galileo concluded "with absolute necessity that Venus revolves about the sun just as do all the other planets", thus consenting to Nicholas Copernicus and Johannes Keppler in discrediting geocentric cosmologies.

which offered a stepwise improved contrast resolution of the echo signals ([1]).

A mathematical cross–correlation analysis of the holographic organizations of synthetic aperture radar data

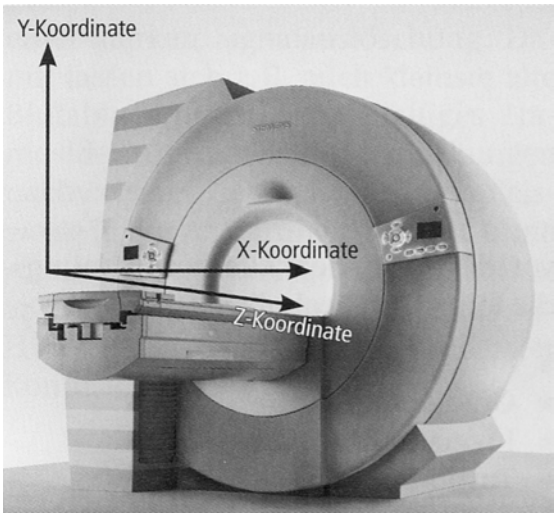

FIGURE 5. Coordinatization procedure in a magnetic resonance tomography scanner by the basis $\{X,Y,Z\}$ of the nilpotent Heisenberg algebra Lie(N), where the vector Z spans the center of Lie(N). The exponential diffeomorphism gives rise to the coordinatization of the three–dimensional real Heisenberg Lie group N by unipotent matrices. The Fourier equivalent polarization planes spanned by $\{X,Z\}$ and $\{Y,Z\}$ in Lie(N) induce the coadjoint orbit picture in the three–dimensioanl real projective space. Modern high end clinical magnetic resonance tomography scanner for routine radiological examinations implement a magnetic field density of 3 Tesla.

leads to harmonic analysis on the Heisenberg group N. The most common synthetic aperture radar mode, the spotlight mode, is operating analogously to the lighthouse model of pulsar astrophysics ([3], [4]). The word pulsar is an acronym based on the phrase "pulsating source of radio emission". The prototypical neutron–star binary pulsar PSR B1913 + 16 at a distance of 21000 light years from the earth cannot be observed by using the visible light even by means of the most sensitive telescopes. The neutron star rotates on its axis 17 times per second. Thus the pulse period is $T = 59$ ms on the time scale. The orbital period of $7\frac{3}{4}$ hours is remarkably short. The pulsar and its companion both follow highly elliptical orbits around their common center of mass. The major axis of the star's orbit is only 6.4 light seconds, and the minor axis is 5 light seconds. Each star moves on its orbit according to the Kepplerian laws of orbital motions. Notice that the eccentric Kepplerian motions are cross–sections of the corotating circular bicylinder passing through the torque ring. It is the image of the projectivized coadjoint orbit picture of the Heisenberg Lie group N under the conformal Möbius inversion.
According to the lighthouse effect, the pulsar's beams of radio waves sweep the earth producing highly regular sequences of radio pulses. The extraordinary stability of the pulse sequences makes pulsars very accurate clocks, rivaling the best atomic clocks on earth, and makes a transversal matched filter bank reconstruction possible. Pulses from the neutron star traverse the interstellar medium before being received at the radio telescope where they are de–dispersed and added to form a mean pulse profile. During the observation, the data regularly receive a time stamp, usually based on a caesium time standard or hydrogen maser at the observatory plus a signal from the global positioning system (GPS) of satellites. The time–of–arrival measurement can be accurately determined by photon cross–correlation of the observed profile with a high signal–to–noise template profile obtained from the linear superposition of many observations at the particular observing frequency label of the filter bank which reconstructs holographically the pulsar's parameters under consideration. The lattice underlying reconstruction procedure leads to the concept of compact Heisenberg nilmanifold which is associated to the Heisenberg Lie group N. It forms a circle bundle over the two–dimensional torus.

3. CLINICAL MAGNETIC RESONANCE TOMOGRAPHY

In clinical magnetic resonance tomography, the symplectic structure of planar cross–sections, called tomographic slices, is used to install the PROPELLER (Periodically Rotated Overlapping ParallEL Lines with Enhanced Reconstruction) strategy of nonuniformly data sampling to mitigate quantum holographically the signal instability present in all multiple–shot fast spin–echo pulse trains. And further, analogously to quantum holographic rotation sensing with a dual atom–interferometer Sagnac gyroscope, the PROPELLER sampling modality of magnetic resonance tomography provides greater immunity of the linear gradient contrast image formation against geometric distortion ([6], [7]).

The clinical utility of diffusion–weighted magnetic resonance tensor imaging is well established ([5], [10]). Few advances in magnetic resonance tomography have had the impact that diffusion–weighted and tensor imaging have had in the evaluation of the human brain. A significant benefit of the PROPELLER sampling modality in high–resolution diffusion–weighted magnetic resonance tensor imaging is its immunity to image warping from eddy currents. The warping phenomenon is a challenge in echo–planar imaging based protocols, since pixels in different regions of the head are warped in a manner that depends on the direction of the diffusion gradient, making image fusion problematic. In the robust PROPELLER sampling modality, tractographic images of fiber pathways corresponding to different diffusion gradient directions are very well registered.

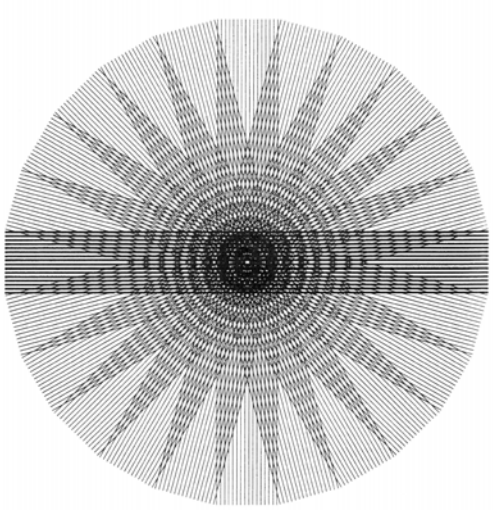

FIGURE 6. Reconstruction procedure of quantum holography for planar signal detectors: The coaxisymmetric data collection trajectory for the metaplectic PROPELLER sampling modality. The bold lines indicate the measured area, called a blade, by one echo train in a fast spin–echo experiment. In subsequent steps, the frequency and phase encode linear gradients are rotated about the tomographic slice selection coaxis. The central core data are resampled for every blade. The data are then combined to the robust formation of a high resolution magnetic resonance tomography contrast image.

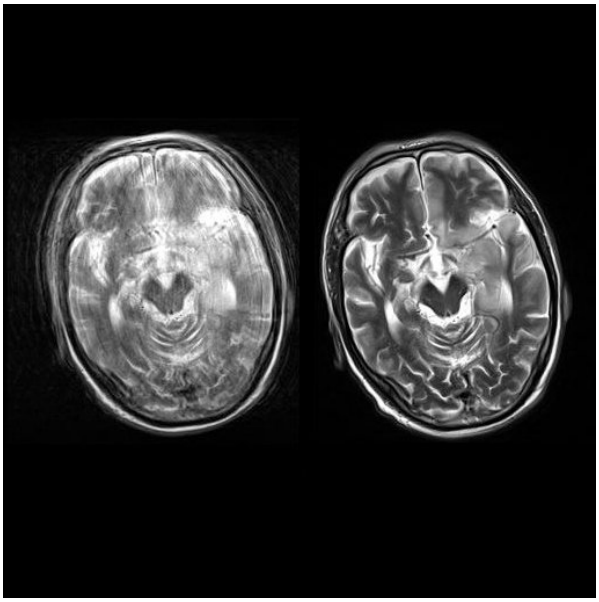

FIGURE 7. Magnetic resonance tomographic image: Transversal slice or axial cross–section of the brain with motion correction. The metaplectic PROPELLER sampling modality reduces dramatically the sensitivity to movement under high resolution magnetic resonance tomographic scanning.

4. BACTERIAL PROTEIN DYNAMICS OF STRUCTURAL MICROBIOLOGY

Bacteria and their genome sequences are evolutionarily and physiologically interesting microbiological objects. Many motile species of bacteria are propelled by flagella, which are rigid helical filaments turned by rotary motors in the cell membrane. The bacterial flagellar motor is a remarkable nanomachine: built from approximately 25 different proteins, it drives the rotation of the helical filaments at speeds of up to 2000 Hz, efficiently propelling bacteria through viscous media. The rotation rates of the flagellar motor had been reported to be, for instance, 170 Hz for *Salmonella typhimurium*, 270 Hz for *Escherichia coli*, and 1700 Hz for *Vibrio alginolyticus*. Indeed, the flagella of *V. alginolyticus* are one of the fastest molecular rotors in biological systems with a pitch of its flagellar helix of 1.58 μm ([2]).

The structure of the bacterial flagellar motor excites considerable interest because of the ordered expression of its genes, its regulated self–assembly, the sophisticated interactions of its proteins, and its startling dynamics. A protein called FliG forms a ring in the spinning rotor of the flagellar motor that is involved in the generation of torque through an interaction with the anion–channel–forming stator proteins MotA and MotB. The latter form a ring of studs within and above the inner membrane that couple the passage of protons across the membrane. A promising application of the sub–Riemannian geometry of the Heisenberg Lie group N is in the bacterial protein dynamics of molecular systems biology. By winding up the Heisenberg helix on the circular bicylinder passing through the torque ring, the central torus singularity and the Galois group $\mathrm{Gal}_{\mathbf{R}}\mathbf{C}$ model in binary terms the molecular structure of the spin switching action on the torque ring in the full–length FliG protein. The Heisenberg helix is a solution of the symplectic Hamilton–Jacobi equations, hence a geodesic trajectory for the sub–Riemannian metric of N.

The diameter of the spinning rotor is about 30 nm. Its flagellas are embedded in the cell surface and constructed by means of about eleven protofilaments of a single protein, *flagellin*. The flagellar motor of peritrichously flagellated bacteria uses the potential energy from an electrochemical gradient of anions across the cytoplasmic membrane to impress angular momentum onto the FliG torque ring. A rapid spin switch from anticlockwise to clockwise rotation determines whether a bacterium runs smoothly forward or tumbles to change its trajectory in response to chemotactic signals. A brief tumble is caused by such a quick reversal of the flagellar motor to clockwise rotation, which generates spin twisting pulses that transforms the left–handed helical path of the filament into a right–handed one. The spin twist can be mod-

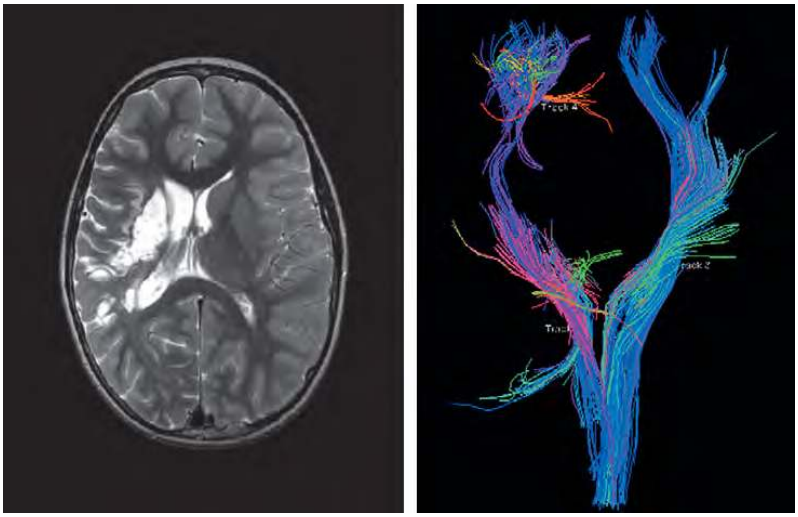

FIGURE 8. Pediatric neuropathology: The morphological magnetic resonance tomographic image demonstrates cystic encephalomalacia and volume loss due to right middle cerebral artey embolic occlusion secondary to traumatic internal carotid artery dissection. The diffusion–weighted magnetic resonance tensor image demonstrates disruption of the major white matter tracts.

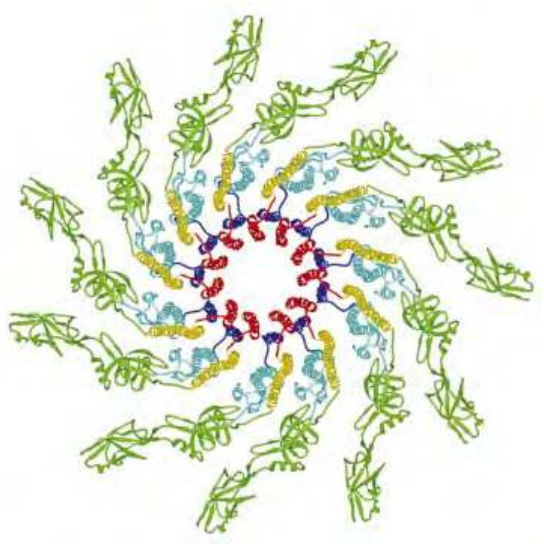

FIGURE 9. Transversal visualization of the flagellin crystal organization: Distal view on the end of the protofilament. Eleven subunits of protofilament and the central core are displayed by the tomographic cryomicroscopic image. The studs are clearly outlined. The spatial resolution is about 2 Å.

elled in binary terms by the action of the Galois group $\mathrm{Gal}_{\mathbf{R}}\mathbf{C}$. Chemotaxis is achieved by modulation of the tumbling frequency. When moving up an attracted gradient, the bacteria encounter an attractant concentration that increases with time. In response, they tumble less frequently and thus continue to move up the gradient. In this way, the analogy to the gradient control of clinical magnetic resonance tomography becomes obvious.

ACKNOWLEDGMENTS

This work has been financially supported by the research project "Geometric analysis of Lie groups amd applications" (GALA) of the European Union.

REFERENCES

1. E.N. Leith, "Synthetic Aperture Radar," in *Optical Data Processing*, edited by D. Casasent, Springer–Verlag, Berlin, Heidelberg, New York, 1978, pp. 89–117.
2. S.A. Lloyd, F.G. Whitby, D.F. Blair, C.P. Hill, *Nature* **400**, 472–476 (1999).
3. D.R. Lorimer, M. Kramer, Handbook of Pulsar Astronomy, Cambridge University Press, Cambridge, New York 2005.
4. A.G. Lyne, F. Graham–Smith, Pulsar Astronomy, Third Edition, Cambridge University Press, Cambridge, New York 2006.
5. T. Moritani, S. Ekholm, P.–L. Westesson, Diffusion–Weighted MR Imaging of the Brain, Second Edition, Springer–Verlag, Berlin, Heidelberg 2009.
6. J.G. Pipe, V.G. Farthing, K.P. Forbes, *Magn. Reson. Med.* **47**, 42–52 (2002).
7. W.J. Schempp, Magnetic Resonance Imaging: Mathematical Foundations and Applications, Wiley–Liss, New York, Chichester, Weinheim 1998.
8. W.J. Schempp, *Math. Meth. Appl. Sci.* **22**, 867–922 (1999).
9. W.J. Schempp, "The Fourier holographic encoding strategy of symplectic spinor visualization," in *New Directions in Holography and Speckles*, edited by H.J. Caulfield, C.S. Vikram, American Scientific Publishers, Stevenson Ranch, California 2008, pp. 479–522.
10. J.D. Schmahmann, D.N. Pandya, Fiber Pathways of the Brain, Oxford University Press, Oxford, New York 2009.